









Research article

UDC 539.3

DOI: 10.34910/MCE.120.3



Stress-strain state of elastic shell based on mixed finite element

Yu.V. Klochkov¹ , V.A. Pshenichkina² , A.P. Nikolaev¹ , O.V. Vakhnina¹  ,
M.Yu. Klochkov² 

¹ Volgograd State Agrarian University, Volgograd, Russian Federation

² Volgograd State Technical University, Volgograd, Russian Federation

✉ ovahnina@bk.ru

Keywords: thin-walled shell-type structure, modified mixed functional, compliance matrix, four-node sampling element, force and kinematic unknowns

Abstract. In a mixed formulation, a four-node finite element was developed, which is a fragment of the middle surface of the elastic shell. Longitudinal forces and bending moments, as well as displacements and their first derivatives with respect to curvilinear coordinates, were taken as nodal unknowns. To obtain the compliance matrix, the Reissner functional was used, in which the stresses, when using the direct normal hypothesis, are represented by dependences on the forces and bending moments of the middle surface, the approximation of which was carried out by bilinear functions. In the interpolating expressions for the kinematic sought quantities, Hermite polynomials of the third degree were used. As a result of minimizing the transformed functional with respect to the force and kinematic nodal unknowns, the compliance matrix of the accepted discrete element was formed. Verification of the developed discrete element in a mixed formulation was carried out on the examples of calculations of cylindrical shells with circular and elliptical cross sections. The values of the force parameters found using the developed algorithm adequately satisfied the conditions of static equilibrium (the calculation error was less than 0.5 %). An analysis of the obtained finite element solutions showed the effectiveness of the developed algorithm and made it possible to note the possibility of its use in calculations of thin-walled structures made of incompressible materials.

Citation: Klochkov, Yu.V., Pshenichkina, V.A., Nikolaev, A.P., Vakhnina, O.V., Klochkov, M.Yu. Stress-strain state of elastic shell based on mixed finite element. Magazine of Civil Engineering. 2023. Article no. 12003. DOI: 10.34910/MCE.120.3

1. Introduction

Definition of the object of the study. The current widespread use of thin-walled shell-type structures (pipelines, tanks, hangars, domed roofs, wide-span ceilings, and others) puts forward a rather urgent task of creating domestic computational algorithms for analyzing the stress-strain state of such technospheric systems and objects.

Literature review. At present, when choosing the optimal shapes and sizes of thin-walled shell-type structures, numerical methods for analyzing their SSS [1–6] come to the fore, with FEM taking the priority position. It is widely used in calculations of plates and shells both under elastic [7–12] and elastoplastic [13, 14] deformation. FEM is essential in the analysis of SSS structures made of composite materials [15–17], as well as in matters of shell stability [18]. Three-dimensional finite elements are used both in the analysis of the stress-strain state of bulk structures and thin-walled structures [19–21].

The relevance of the research. Most of the currently created finite element computing systems are based on FEM in the formulation of the displacement method, which inevitably leads to the need to calculate second-order partial derivatives of the normal component of the displacement vector when using the theory of thin shells [22] based on the Kirchhoff-Love hypotheses. At the same time, finite element algorithms for

determining the stress-strain state of shell structures in a mixed formulation [23, 24] make it possible to obtain the desired internal force quantities (longitudinal forces and bending moments) directly in the process of solving the system of equations formed as a result of minimizing the mixed Reissner functional. This can also be achieved without organizing additional computational procedures that greatly complicate the finite element algorithm for calculating thin-walled shell-type structures.

The purpose and objectives of the study. This paper presents the derivation of the modified Reissner functional, in which the total specific work of stresses is expressed in terms of the specific work of longitudinal forces and bending moments at a point of the middle surface on deformations and curvatures of the middle surface at this point. By minimizing the modified mixed functional with respect to force (longitudinal forces and bending moments) and kinematic (displacement vector components and their first-order partial derivatives) nodal unknowns, the compliance matrix and the column of nodal forces of a quadrangular discretization element, which is a fragment of the middle surface of a thin-walled shell-type structure, are assembled.

The verification of the developed algorithm was carried out on the example of determining the SSS of cylindrical shells with circular and elliptical cross sections. An analysis of the results of the obtained finite element solutions made it possible to conclude that the developed algorithm is effective and that the calculation accuracy of the required force and kinematic nodal unknowns is acceptable.

2. Materials and Methods

The median surface of a thin-walled shell-type structure can be given by the radius vector

$$\vec{R}^0 = x\vec{i} + y(x, t)\vec{j} + z(x, t)\vec{k}, \quad (1)$$

where t is a parameter counted from the vertical axis in a plane perpendicular to the axis Ox , which is at a distance of x from the origin.

Basis vectors of a point M^0 are determined by derivatives

$$\vec{a}_1^0 = \vec{R}_{,x}^0; \quad \vec{a}_2^0 = \vec{R}_{,t}^0; \quad \vec{a}^0 = \vec{a}_1^0 \times \vec{a}_2^0 / \sqrt{a_0}, \quad (2)$$

where $a_0 = (\vec{a}_1^0 \cdot \vec{a}_1^0)(\vec{a}_2^0 \cdot \vec{a}_2^0) - (\vec{a}_1^0 \cdot \vec{a}_2^0)^2$.

The derivatives of the basis vectors of point M^0 are determined by the components in the same basis [25]

$$\vec{a}_{\alpha,\beta}^0 = \Gamma_{\alpha\beta}^{0\rho} \vec{a}_\rho^0 + b_{\alpha\beta}^0 \vec{a}^0; \quad \vec{a}_{,\beta}^0 = -b_{\beta}^{0\rho} \vec{a}_\rho^0, \quad (3)$$

where indices α, β, ρ take values 1, 2; $\Gamma_{\alpha\beta}^{0\rho}$ are Christoffel symbols of the second kind; $b_{\beta}^{0\rho}$ are mixed components of the curvature tensor.

The position of the point of the shell at a distance of ζ from the point of the middle surface M^0 , as well as its position after the application of a given load, are determined by the radius vectors

$$\vec{R}^{0\zeta} = \vec{R}^0 + \zeta \vec{a}^0; \quad \vec{R}^\zeta = \vec{R}^{0\zeta} + \vec{V}. \quad (4)$$

The displacement vector \vec{V} of point $M^{0\zeta}$ according to the direct normal hypothesis [22] can be represented by the following expression

$$\vec{V} = \vec{v} + \zeta (\vec{a} - \vec{a}^0), \quad (5)$$

where $\vec{v} = v^\rho \vec{a}_\rho^0 + v \vec{a}^0$ is the displacement vector of point $M^{0\zeta}$; $\vec{a} = \vec{a}_1 \times \vec{a}_2 / \sqrt{a}$ is unit vector of the normal at point M ; $\vec{a}_\rho = \vec{a}_\rho^0 + \vec{v}_{,\rho}$ are covariant vectors of the local basis of point M of the deformed state.

Here and below, the comma means the operation of differentiation with respect to global coordinates x and t .

The basis vectors of points $M^{0\zeta}$ and M^ζ are determined by the corresponding differentiation (4) with respect to x and t

$$\vec{g}_p^0 = \vec{R}_{,p}^{0\zeta} = \vec{a}_p^0 - \zeta b_p^{0\gamma} \vec{a}_\gamma^0; \quad \vec{g}_p = \vec{R}_{,p}^\zeta = \vec{g}_p^0 + \vec{v}_{,p} + \zeta (\vec{a}_{,p} - b_p^{0\gamma} \vec{a}_\gamma^0). \quad (6)$$

Deformations at point M^ζ of a thin-walled shell-type structure are determined by the difference between the components of the metric tensors at the point of the initial and deformed states [26]

$$\varepsilon_{p\gamma}^\zeta = (g_{p\gamma} - g_{p\gamma}^0) / 2. \quad (7)$$

Four-node element. The finite element is represented by a quadrangular part of the middle surface with nodes i, j, k, l . Taking into account that when implementing the mixed formulation of the FEM, there is no need to include the desired unknown higher-order derivatives in the structure, the column of nodal variable parameters of the used quadrangular sampling element in the local $-1 \leq \xi, \eta \leq 1$ and global x, t coordinate systems was chosen in the form

$$\left\{ U^L \right\}_{1 \times 60}^T = \left\{ \left\{ N \right\}_{1 \times 12}^T \left\{ M \right\}_{1 \times 12}^T \left\{ v^{1L} \right\}_{1 \times 12}^T \left\{ v^{2L} \right\}_{1 \times 12}^T \left\{ v^L \right\}_{1 \times 12}^T \right\}; \quad (8)$$

$$\left\{ U^G \right\}_{1 \times 60}^T = \left\{ \left\{ N \right\}_{1 \times 12}^T \left\{ M \right\}_{1 \times 12}^T \left\{ v^{1G} \right\}_{1 \times 12}^T \left\{ v^{2G} \right\}_{1 \times 12}^T \left\{ v^G \right\}_{1 \times 12}^T \right\}, \quad (9)$$

where $\left\{ N \right\}_{1 \times 12}^T = \left\{ N^{11i} N^{11j} N^{11k} N^{11l} N^{22i} \dots N^{22l} N^{12i} \dots N^{12l} \right\};$

$\left\{ M \right\}_{1 \times 12}^T = \left\{ M^{11i} M^{11j} M^{11k} M^{11l} M^{22i} \dots M^{22l} M^{12i} \dots M^{12l} \right\}$ are columns of power parameters;

$\left\{ q^L \right\}_{1 \times 12}^T = \left\{ q^i q^j q^k q^l q_\xi^i \dots q_{,\xi}^l q_{,\eta}^i \dots q_{,\eta}^l \right\}; \quad \left\{ q^G \right\}_{1 \times 12}^T = \left\{ q^i q^j q^k q^l q_{,x}^i \dots q_{,x}^l q_{,t}^i \dots q_{,t}^l \right\}$ are columns of

kinematic parameters in local $-1 \leq \xi, \eta \leq 1$ and global x, t coordinate systems, respectively.

Here, q means the values v^p, v .

Bilinear functions of local coordinates ξ, η [27] were used as shape functions for the force unknowns

$$N^{\alpha\beta} = \left\{ \varphi \right\}_{1 \times 4}^T \left\{ N^{\alpha\beta} \right\}_{4 \times 1}; \quad M^{\alpha\beta} = \left\{ \varphi \right\}_{1 \times 4}^T \left\{ M^{\alpha\beta} \right\}_{4 \times 1}, \quad (10)$$

and for the kinematic required unknowns, the products of Hermite polynomials of the third order were applied [27]

$$q = \left\{ \psi \right\}_{1 \times 12}^T \left\{ q^L \right\}_{12 \times 1}. \quad (11)$$

Compliance matrix of a four-node bin. To obtain the compliance matrix of a four-node discretization element, one can use the Reissner functional written in the following form

$$\Pi_S = \int_V \left\{ \sigma^{p\gamma} \right\}^T \left\{ \varepsilon_{p\gamma}^\zeta \right\} dV - 0.5 \int_V \left\{ \sigma^{p\gamma} \right\}^T [C] \left\{ \sigma^{p\gamma} \right\} dV - 0.5 \int_F \left\{ U \right\}^T \left\{ P \right\} dF, \quad (12)$$

where $\{\sigma^{p\gamma}\}^T = \{\sigma^{11}\sigma^{22}\sigma^{12}\}$; $\{\varepsilon^{p\gamma}\}^T = \{\varepsilon_{11}^\zeta \varepsilon_{22}^\zeta 2\varepsilon_{12}^\zeta\}$; $\{U\}^T = \{v^1 v^2 v\}$; $\{P\}^T = \{p^1 p^2 p\}$ is column of the external surface load vector.

In accordance with [26], the elasticity matrix $[C]$ included in (12) determines the relationship between columns $\{\varepsilon_{p\gamma}^\zeta\}$ and $\{\sigma^{p\gamma}\}$

$$\{\varepsilon_{p\gamma}^\zeta\} = [C] \{\sigma^{p\gamma}\}. \quad (13)$$

Column $\{\sigma^{p\gamma}\}$, on the basis of the theory of thin shells [22], can be expressed in terms of the required force unknowns, which are the longitudinal forces $N^{\alpha\beta}$ and bending moments $M^{\alpha\beta}$

$$\{\sigma^{p\gamma}\}_{3 \times 1} = [D_\sigma]_{3 \times 6} \{NM\}_{6 \times 1}, \quad (14)$$

$$\text{where } [D_\sigma]_{3 \times 6} = \begin{bmatrix} 1/h & 0 & 0 & \zeta/I & 0 & 0 \\ 0 & 1/h & 0 & 0 & \zeta/I & 0 \\ 0 & 0 & 1/h & 0 & 0 & \zeta/I \end{bmatrix}; \quad \{NM\}^T = \{N^{11} N^{22} N^{12} M^{11} M^{22} M^{12}\}; \quad h \text{ is}$$

the shell thickness; $I = h^3/12$ is moment of inertia.

The column of covariant components of the strain tensor at point M^ζ , taking into account the direct normal hypothesis [22], Cauchy relations (7), and interpolation dependence (11), can be represented by the matrix relation

$$\{\varepsilon_{p\gamma}^\zeta\}_{3 \times 6} = [D_\varepsilon]_{3 \times 6} \{\varepsilon_{p\gamma}\}_{6 \times 1} = [D_\varepsilon]_{3 \times 6} [B]_{3 \times 36} \{u^L\}_{36 \times 1} = [D_\varepsilon]_{3 \times 6} [B]_{3 \times 36} [T]_{36 \times 36} \{u^G\}_{36 \times 1}, \quad (15)$$

$$\text{where } [D_\varepsilon]_{3 \times 6} = \begin{bmatrix} 1 & 0 & 0 & \zeta & 0 & 0 \\ 0 & 1 & 0 & 0 & \zeta & 0 \\ 0 & 0 & 1 & 0 & 0 & \zeta \end{bmatrix}; \quad \{\varepsilon^{p\gamma}\}_{1 \times 6}^T = \{\varepsilon_{11} \varepsilon_{22} 2\varepsilon_{12} \mathfrak{N}_{11} \mathfrak{N}_{22} 2\mathfrak{N}_{12}\}$$
 is a column of

deformations and curvatures at point M of the middle surface; $\{u^L\}_{1 \times 36}^T = \left\{ \begin{matrix} \{v^{1L}\}^T & \{v^{2L}\}^T & \{v^L\}^T \\ 1 \times 12 & 1 \times 12 & 1 \times 12 \end{matrix} \right\}$;

$\{u^G\}_{1 \times 36}^T = \left\{ \begin{matrix} \{v^{1G}\}^T & \{v^{2G}\}^T & \{v^G\}^T \\ 1 \times 12 & 1 \times 12 & 1 \times 12 \end{matrix} \right\}$; $[T]$ is transformation matrix of the column of kinematic quantities

from the local coordinate system ξ, η to the global one x, t .

The column of power variable parameters $\{NM\}$ is interpolated through its nodal values using relations (10)

$$\{NM\}_{6 \times 1} = [H]_{6 \times 24} \{G^{\alpha\beta}\}_{24 \times 1}, \quad (16)$$

$$\text{where } \{G^{\alpha\beta}\}_{24 \times 1}^T = \left\{ \begin{matrix} \{N^{11}\}^T & \{N^{22}\}^T & \{N^{12}\}^T & \{M^{11}\}^T & \{M^{22}\}^T & \{M^{12}\}^T \\ 1 \times 4 & 1 \times 4 & 1 \times 4 & 1 \times 4 & 1 \times 4 & 1 \times 4 \end{matrix} \right\}.$$

Functional (12), taking into account (14) and (16), can be represented as

$$\begin{aligned} \Pi_S = & \left\{ G^{\alpha\beta} \right\}_{1 \times 24}^T \int_V \left[H \right]_{24 \times 6}^T \left[D_\sigma \right]_{6 \times 3}^T \left[D_\varepsilon \right]_{3 \times 6} \left[B \right]_{6 \times 36} dV \left[T \right]_{36 \times 36} \left\{ u^G \right\}_{36 \times 1} - \\ & - 0.5 \left\{ G^{\alpha\beta} \right\}_{1 \times 24}^T \int_V \left[H \right]_{24 \times 6}^T \left[D_\sigma \right]_{6 \times 3}^T \left[C \right]_{3 \times 3} \left[D_\sigma \right]_{3 \times 6} \left[H \right]_{6 \times 24} dV \left\{ G^{\alpha\beta} \right\}_{24 \times 1} - \\ & - 0.5 \left\{ u^G \right\}_{1 \times 36}^T \left[T \right]_{36 \times 36}^T \int_F \left[A \right]_{36 \times 3}^T \left\{ P \right\}_{3 \times 1} dF, \end{aligned} \quad (17)$$

$$\text{where } [A] = \begin{bmatrix} \left\{ \psi \right\}_{1 \times 12}^T & 0 & 0 \\ 0 & \left\{ \psi \right\}_{1 \times 12}^T & 0 \\ 0 & 0 & \left\{ \psi \right\}_{1 \times 12}^T \end{bmatrix}_{3 \times 36}.$$

Applying to (17) the procedure of minimization with respect to the required unknowns $\left\{ G^{\alpha\beta} \right\}^T$, we can obtain the following matrix expression

$$\partial \Pi_S / \partial \left\{ G^{\alpha\beta} \right\}^T = [S]_{24 \times 36} \left\{ u^G \right\}_{36 \times 1} - [Z]_{24 \times 24} \left\{ G^{\alpha\beta} \right\}_{24 \times 1} = 0, \quad (18)$$

$$\text{where } [S] = \int_V \left[H \right]_{24 \times 6}^T \left[D_\sigma \right]_{6 \times 3}^T \left[D_\varepsilon \right]_{3 \times 6} \left[B \right]_{6 \times 36} dV [V]; \quad [Z] = \int_V \left[H \right]_{24 \times 6}^T \left[D_\sigma \right]_{6 \times 3}^T \left[C \right]_{3 \times 3} \left[D_\sigma \right]_{3 \times 6} \left[H \right]_{6 \times 24} dV.$$

The first integral in functional (12) can be represented in the following form

$$\begin{aligned} \int_V \left\{ \sigma^{\rho\gamma} \right\}_{1 \times 3} \left\{ \varepsilon_{\rho\gamma}^\zeta \right\}_{3 \times 1} dV &= \int_V \left\{ \varepsilon_{\rho\gamma}^\zeta \right\}_{1 \times 3}^T \left\{ \sigma^{\rho\gamma} \right\}_{3 \times 1} dV = \\ &= \left\{ u^G \right\}_{1 \times 36}^T \left[T \right]_{36 \times 36}^T \int_V \left[B \right]_{36 \times 6}^T \left[D_\varepsilon \right]_{6 \times 3}^T \left[D_\sigma \right]_{3 \times 6}^T \left[H \right]_{6 \times 24} dV \left\{ G^{\alpha\beta} \right\}_{24 \times 1}. \end{aligned} \quad (19)$$

By minimizing the functional (17) taking into account (19) with respect to the kinematic unknown unknowns $\left\{ u^G \right\}^T$, we can write the following matrix relation

$$\partial \Pi_S / \partial \left\{ u^G \right\}^T = [S]_{36 \times 24}^T \left\{ G^{\alpha\beta} \right\}_{24 \times 1} - \left\{ R \right\}_{36 \times 1} = 0, \quad (20)$$

$$\text{where } \left\{ R \right\} = \left[T \right]^T \int_F \left[A \right]^T \left\{ P \right\} dF.$$

The system of equations obtained as a result of minimizing the functional Π_S with respect to $\left\{ G^{\alpha\beta} \right\}^T$ and $\left\{ u^G \right\}^T$ can be represented in the matrix form

$$\begin{bmatrix} - [Z]_{24 \times 24} & [S]_{24 \times 36} \\ [S]_{36 \times 24}^T & [0]_{36 \times 36} \end{bmatrix} \begin{bmatrix} \left\{ G^{\alpha\beta} \right\}_{24 \times 1} \\ \left\{ u^G \right\}_{36 \times 1} \end{bmatrix} = \begin{bmatrix} \left\{ 0 \right\}_{24 \times 1} \\ \left\{ R \right\}_{36 \times 1} \end{bmatrix} \quad (21)$$

or in a more compact form

$$\begin{bmatrix} K \end{bmatrix}_{60 \times 60} \begin{Bmatrix} U^G \end{Bmatrix}_{60 \times 1} = \begin{Bmatrix} f \end{Bmatrix}_{60 \times 1}, \quad (22)$$

where $\begin{bmatrix} K \end{bmatrix}_{60 \times 60} = \begin{bmatrix} -[Z]_{24 \times 24} & [Z]_{24 \times 36} \\ [S]^T_{36 \times 24} & [0]_{36 \times 36} \end{bmatrix}$ is the flexibility matrix of a four-node sampling element; $\begin{Bmatrix} f \end{Bmatrix}_{1 \times 60}^T = \begin{Bmatrix} \{0\}^T_{1 \times 24} & \{R\}^T_{1 \times 36} \end{Bmatrix}$ is column of nodal forces.

An analysis of the structures of matrices $[Z]$ and $[S]$ in the compliance matrix $[K]$ shows that matrix $[K]$ is also a determinable value in the case of an incompressible material at a transverse strain coefficient of $\nu = 0.5$.

Analyzing the resulting compliance matrix $[K]$, it can be noted that it contains a significant zero block $[0]_{36 \times 36}$, which can significantly reduce the conditionality of the global compliance matrix of the entire shell-type structure. To eliminate this problem, this paper proposes to carry out the following transformations.

Let us express from equation (18) the column of force nodal unknowns

$$\begin{Bmatrix} G^{\alpha\beta} \end{Bmatrix}_{24 \times 1} = \begin{bmatrix} Z \end{bmatrix}_{24 \times 24}^{-1} \begin{bmatrix} S \end{bmatrix}_{24 \times 36} \begin{Bmatrix} u^G \end{Bmatrix}_{36 \times 1} \quad (23)$$

and substitute relation (23) into equation (20)

$$\begin{bmatrix} S \end{bmatrix}_{36 \times 24}^T \begin{bmatrix} Z \end{bmatrix}_{24 \times 24}^{-1} \begin{bmatrix} S \end{bmatrix}_{24 \times 36} \begin{Bmatrix} u^G \end{Bmatrix}_{36 \times 1} - \begin{Bmatrix} R \end{Bmatrix}_{36 \times 1} = 0. \quad (24)$$

Transforming (24), we can obtain the following matrix expression

$$\begin{bmatrix} L \end{bmatrix}_{36 \times 36}^T = \begin{Bmatrix} u^G \end{Bmatrix}_{36 \times 1} = \begin{Bmatrix} R \end{Bmatrix}_{36 \times 1}, \quad (25)$$

where $\begin{bmatrix} L \end{bmatrix}_{36 \times 36} = \begin{bmatrix} S \end{bmatrix}_{36 \times 24}^T \begin{bmatrix} Z \end{bmatrix}_{24 \times 24}^{-1} \begin{bmatrix} S \end{bmatrix}_{24 \times 36}$ is the modified compliance matrix of the four-node bin.

Analyzing (25), it can be noted that $\begin{bmatrix} L \end{bmatrix}_{36 \times 36}$ does not contain a zero block and differs from $\begin{bmatrix} K \end{bmatrix}_{60 \times 60}$ in a significantly smaller dimension, which reduces the requirements for the amount of RAM used by computer equipment when studying the stress-strain state of a thin-walled shell-type structure.

Based on the obtained modified compliance matrix $\begin{bmatrix} L \end{bmatrix}_{36 \times 36}$, with the help of the index matrix [28], the global compliance matrix of the entire calculated thin-walled shell-type structure is assembled and the solution of the global system of algebraic equations is performed, the unknowns of which are only the kinematic nodal unknowns $\begin{Bmatrix} u^G \end{Bmatrix}$.

After calculating the kinematic nodal unknowns $\begin{Bmatrix} u^G \end{Bmatrix}$ using (23), without any difficulty, one can obtain the values of the desired force unknowns at any point of interest to the designer in the considered thin-walled shell-type structure.

Verification of the developed computational algorithm based on the use of the modified compliance matrix of the four-node discretization element $[L]_{36 \times 36}$ was performed on specific calculation examples.

3. Results and Discussion

Calculation example 1. As a test example, a circular cylinder was calculated, rigidly clamped on the right end and having a free edge on the left end. The radius vector (1) in this case will look like

$$\vec{R}^0 = x\vec{i} + R \sin t \vec{j} + R \cos t \vec{k}. \quad (26)$$

The cylinder was loaded with an internal pressure of intensity q_w and a uniformly distributed axial load q_u applied along the free left end. The design scheme of the shell is shown in Fig. 1.

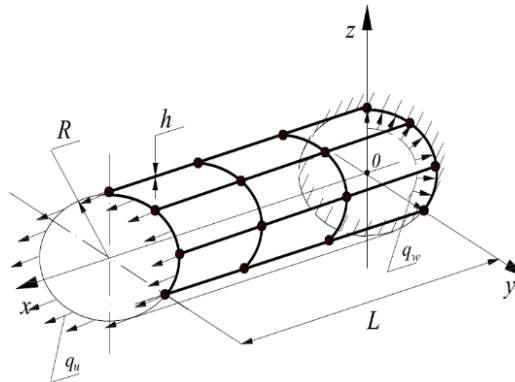


Figure 1. Calculation scheme of a circular cylinder with a uniformly distributed axial load q_u and internal pressure q_w .

The following initial values are accepted: $R = 0.9$ m; $h = 0.02$ m; $L = 0.8$ m; $E = 2 \cdot 10^5$ MPa; $\nu = 0.3$; $q_w = 5$ MPa; $q_u = 500$ kN/m.

The values of stresses in the edge sections of the shell are presented in Table 1 for various variants of discretization of the shell fragment, considered according to the symmetry conditions.

Table 1. Stress values in sections of a cylindrical shell.

Characteristic section	Stress, MPa	Grid of Discretization Nodes				Analytical Solution
		21x21	41x41	51x51	61x61	
Rigid termination	σ_{11}^{in}	410.5	417.5	418.3	418.8	–
	σ_{11}^{out}	–360.5	–367.5	–368.3	–368.8	–
	σ_{11}^{midl}	25.00	25.00	25.00	25.00	25.00
	σ_{22}^{in}	117.5	122.3	123.0	123.3	–
	σ_{22}^{out}	–113.7	–113.1	–113.0	–112.9	–
	σ_{22}^{midl}	4.48	7.24	7.62	7.84	–
Free end	σ_{11}^{in}	24.98	24.99	25.00	25.00	–
	σ_{11}^{out}	25.02	25.01	25.00	25.00	–
	σ_{11}^{midl}	25.00	25.00	25.00	25.00	25.00
	σ_{22}^{in}	226.8	226.8	226.8	226.8	–
	σ_{22}^{out}	222.0	222.0	222.0	222.0	–
	σ_{22}^{midl}	224.5	224.5	224.5	224.5	225.0

An analysis of the data presented in Table 1 allows us to state the fact of a fairly fast convergence of the computational process as the grid of discretization nodes thickens. In addition, it should be noted that the numerical values of normal stresses correspond to the physical meaning of the problem being solved. Meridional stresses σ_{11} on the middle surface in the outer and inner fibers of the edge sections of the cylindrical shell correspond to a given axial external load

$$\sigma_{11}^{midl} = q_u/h = 500 \text{ kN/m}/0.02 \text{ m} = 25.0 \text{ MPa.}$$

Ring stresses of the middle surface at the free end of the cylinder $\sigma_{22}^{midl} = 224.5 \text{ MPa}$ correspond to the specified internal pressure q_w with an acceptable level of error $\delta = 0.22 \%$.

$$\sigma_{22}^{midl} = \frac{q_w \cdot R}{h} = \frac{5 \text{ MPa} \cdot 0.9 \text{ m}}{0.02 \text{ m}} = 225.0 \text{ MPa.}$$

The developed algorithm for determining the stress-strain state of thin shells, which implements a mixed version of the FEM, makes it possible to immediately obtain internal force factors (longitudinal forces and bending moments) at any point of the shell structure of interest to the researcher without excessive labor-intensive calculations. "Physical" values of forces and moments in the edge sections of the cylindrical shell, referred to the middle surface, are presented in Table 2, the structure of which is similar to Table 1.

Table 2. Values of forces and moments in a circular cylinder.

Characteristic section	Efforts, N; moments, N · m	Grid of discretization nodes				Analytical Solution
		21×21	41×41	51×51	61×61	
Rigid termination	N_{11}	500.0	500.0	500.0	500.0	500.0
	N_{22}	89.7	144.7	152.5	156.8	–
	M_{11}	–2570.0	–2616.6	–2622.3	–2625.4	–
	M_{22}	–771.2	–785.8	–787.6	–788.6	–
Free end	N_{11}	500.0	500.0	500.0	500.0	500.0
	N_{22}	4490.5	4490.3	4490.3	4490.3	4500.0
	M_{11}	0.131	0.035	0.023	0.016	0.000
	M_{22}	–49.3	–49.3	–49.3	–49.3	–

The data in Table 2 testify to the stable convergence of the computational process in terms of forces and moments. The values of the axial longitudinal forces N_{11} in the edge sections of the cylindrical shell correspond to a given axial load of $q_u = 500 \text{ kN/m}$. The value of the longitudinal ring force also corresponds to a given internal pressure q_w with a minimum error $\delta = 0.2 \%$.

The bending moment M_{11} tends monotonically to zero in the end section.

On the basis of the foregoing, it can be concluded that the developed algorithm is correct and that the accuracy of calculating the controlled strength parameters of the SSS of shell structures is sufficient for engineering practice.

Calculation example 2. The stress-strain state of a cylindrical shell with an elliptical cross section, rigidly fixed at the ends, loaded with an internal pressure of $q = 5 \text{ MPa}$ is determined. Due to the presence of symmetry, 1/8 of the shell was considered. The design scheme is shown in Fig. 2.

Characteristic section	Stress, MPa; moments, N•m	Grid of discretization nodes					Solution in the formulation of the displacement method, 61x61
		41x41	51x51	61x61	81x81	101x101	
Mid-span, $x = L / 2;$ $t = \pi / 2$ rad. (point D)	σ_{11}^{in}	37.72	37.72	37.73	37.73	37.73	37.84
	σ_{11}^{out}	9.81	9.81	9.81	9.81	9.81	9.83
	σ_{22}^{in}	173.9	173.9	174.0	174.0	174.0	174.7
	σ_{22}^{out}	144.2	144.2	144.2	144.3	144.3	144.8

As follows from the analysis of tabular data, the convergence of the computational process in terms of both stresses and moments is very stable. In order to verify the developed algorithm, the rightmost column contains the stress values found based on the use of a quadrangular finite element, the stiffness matrix of which was composed on the basis of a finite element procedure in the formulation of the displacement method [27]. As shown by a comparative analysis of the finite element solutions obtained on the basis of the developed algorithm, and the FEM in the formulation of the displacement method, the numerical values of the normal stresses practically coincide at all characteristic points with an acceptable minimum discrepancy in the values of σ_{22} at points A and B. When performing this comparative analysis one should take into account the fact that when implementing the developed algorithm in a mixed formulation, it is possible to directly obtain the numerical values of force factors (forces and moments) and stresses at any of the nodal points of the calculated shell. When using FEM in the formulation of the displacement method, to obtain numerical values of stresses, it is required to perform several stages of computational procedures, namely: after obtaining the displacement values and their first derivatives, it is necessary to calculate the values of the second derivatives of the normal displacement using an interpolation procedure. Then, using the Cauchy relation [22], it is necessary to calculate the deformations of the midsurface point. Next, it is necessary to proceed, on the basis of the Kirchhoff-Love hypotheses, to deformations at a point of an arbitrary layer of the shell, and only after that, using the relations of Hooke's law, it is possible to obtain the stress values. All the above computational procedures complicate the calculation algorithm and increase the calculation error. The use of a mixed formulation of the FEM implemented in the developed algorithm makes it possible to avoid additional cumbersome computational procedures and makes it possible to directly obtain the desired strength parameters of the calculated shell structure, which ultimately makes the developed algorithm the most preferable in the analysis of SSS of shell structures of various configurations.

Calculation example 3. The quadrangular discretization element developed in this work in a mixed formulation can be effectively used to study the SSS of shells made of an incompressible material. The problem was solved to determine the strength parameters of an elliptical cylinder, the design scheme, the geometric and physical characteristics of which coincide with the data of calculation example 2. The difference was that Poisson's ratio was taken equal to $\nu = 0.5$, i.e. it was assumed that the shell is made of an incompressible material. The results of the numerical experiment are presented in tabular and graphical forms. Table No. 4, the structure of which is similar to the structure of Table No. 3, presents the numerical values of normal stresses and bending moments in the support and span sections of an elliptical cylinder, depending on the degree of refinement of the grid of discretization nodes of the calculated shell fragment. Analyzing the tabular data, one can state the stable convergence of the computational process as the grid of discretization nodes becomes denser.

Table 4. Values of normal stresses and bending moments in an elliptical cylinder made of incompressible material.

Characteristic section	Stress, MPa; moments, N•m	Grid of discretization nodes				
		41x41	51x51	61x61	81x81	101x101
Rigid termination, $x = 0.0$; $t = 0.0$ rad. (point A)	σ_{11}^{in}	689.8	690.0	690.1	690.2	690.3
	σ_{11}^{out}	-493.3	-493.5	-493.6	-493.7	-493.8
	σ_{22}^{in}	334.4	336.0	337.1	338.4	339.1
	σ_{22}^{out}	-257.0	-255.6	-254.7	-253.6	-252.9
	M_{11}	-394.3	-394.5	-394.6	-394.6	-394.7
	M_{22}	-197.6	-197.7	-197.8	-197.8	-197.8
Rigid termination, $x = 0.0$; $t = \pi / 2$ rad. (point B)	σ_{11}^{in}	247.8	248.1	248.3	248.5	248.6
	σ_{11}^{out}	-41.27	-41.60	-41.77	-41.95	-42.03
	σ_{22}^{in}	129.5	128.3	127.4	126.3	125.7
	σ_{22}^{out}	-14.97	-16.52	-17.55	-18.83	-19.60
	M_{11}	-96.36	-96.57	-96.69	-96.81	-96.86
	M_{22}	-49.39	-49.47	-49.51	-49.55	-49.56
Mid-span, $x = L / 2$; $t = 0.0$ rad. (point C)	σ_{11}^{in}	108.7	108.7	108.7	108.7	108.7
	σ_{11}^{out}	156.3	156.3	156.3	156.3	156.3
	σ_{22}^{in}	305.4	305.4	305.4	305.4	305.4
	σ_{22}^{out}	347.3	347.2	347.2	347.2	347.2
Mid-span, $x = L / 2$; $t = \pi / 2$ rad. (point D)	σ_{11}^{in}	73.92	73.92	73.92	73.91	73.91
	σ_{11}^{out}	34.0	34.0	34.0	34.0	34.0
	σ_{22}^{in}	179.4	179.4	179.4	179.5	179.5
	σ_{22}^{out}	139.2	139.2	139.3	139.3	139.3

Fig. 3 shows the graphs of changes in normal stresses on the inner σ^{in} and outer σ^{out} surfaces of the shell, as well as bending moments M_{11} , M_{22} on the middle surface along the generatrix of the elliptical cylinder.

The analysis of the graphical material shows that the maximum values of the edge effect appear directly in the rigid embedment, gradually fading towards the zone located at a distance of $0.1 L$ from the reference section, which corresponds to the physical meaning of the problem being solved.

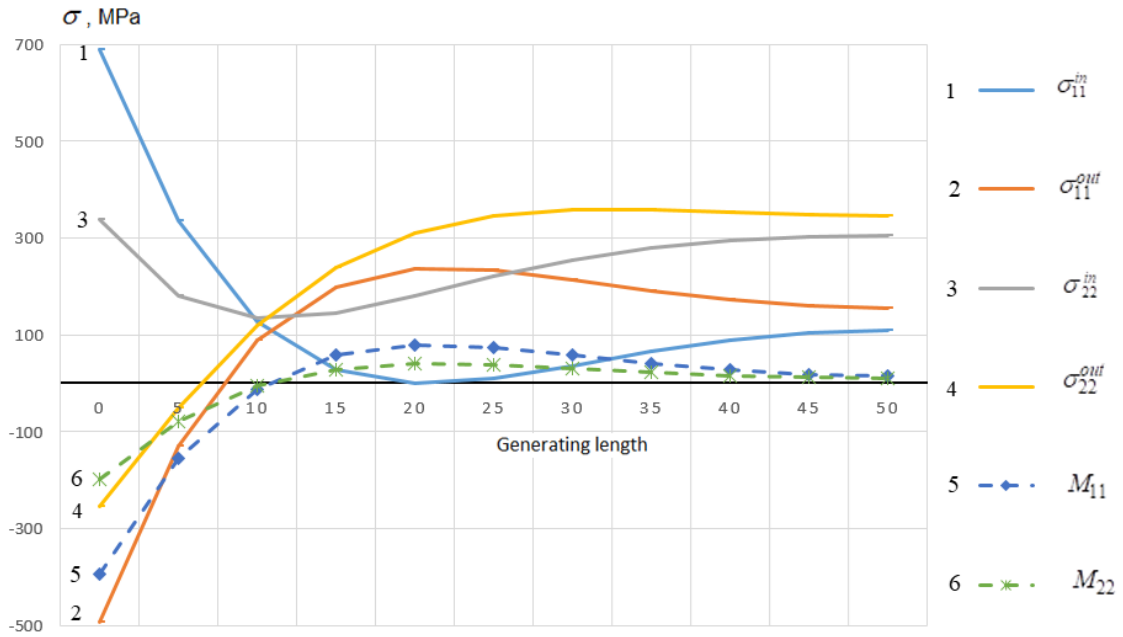


Figure 3. Diagrams of normal stresses and bending moments along the generatrix at $t = 0.0$ rad.

Fig. 4 shows the changes in the normal stresses σ^{in} and σ^{out} , as well as the bending moment M_{11} , M_{22} along the arc of the shell cross section in a rigid enclosure ($x = 0.0$ m).

Analyzing the graphs presented in Figure 4, it can be noted that the controlled strength characteristics (normal stresses and bending moments) reach a maximum at the value of parameter t equal to zero. Then the values of normal stresses and bending moments gradually decrease (by about two times) to their minimum values in the reference section at the value of parameter t equal to $\pi/2$.

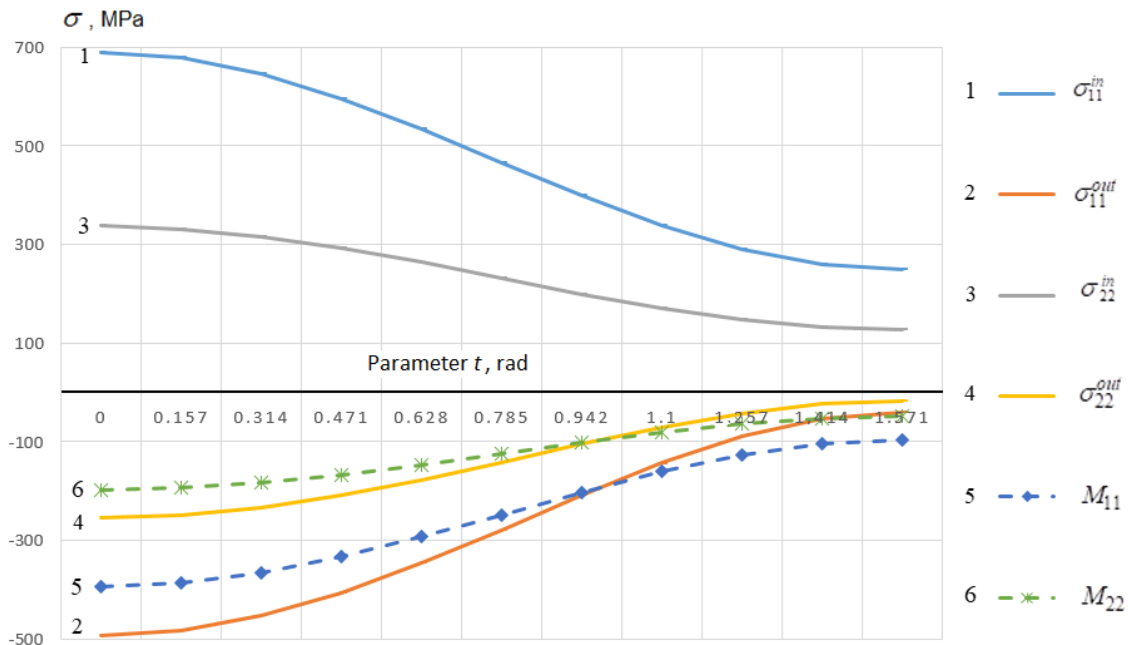


Figure 4. Diagrams of normal stresses and bending moments in rigid termination at $x = 0.0$ m.

4. Conclusions

Taking into account the results of the numerical studies, we can draw the following conclusions.

1. The convergence of the computational process using the developed finite element in a mixed formulation is stable in terms of both force and kinematic factors.

2. The obtained numerical values of the stresses at the controlled points are in adequate agreement with the stress values found from the conditions of static equilibrium (the calculation error does not exceed 0.5 %).

3. The use of the developed mixed finite element leads to the possibility of determining the power parameters directly as a result of solving the system of resolving equations.

4. The developed finite element in a mixed formulation is suitable for determining the SSS of thin-walled structures made of incompressible materials ($\nu = 0.5$).

References

1. Krysko, A.V., Awrejcewicz, J., Bodyagina, K.S., Zhigalov, M.V., Krysko, V.A. Mathematical Modeling of Physically Nonlinear 3D Beams and Plates Made of Multimodulus Materials. *Acta Mechanica*. 2021. 232 (2). Pp. 3441–3469. DOI: 10.1007/s00707-021-03010-8
2. Storozhuk, E.A. Stress–Strain State and Stability of a Flexible Circular Cylindrical Shell with Transverse Shear Strains. *International Applied Mechanics*. 2021. 57 (5). Pp. 554–567. DOI: 10.1007/s10778-021-01106-1
3. Abroso, Y.Y., Maximyuk, V.A., Chernyshenko, I.S. Physically Nonlinear Deformation of a Long Orthotropic Cylindrical Shell with Elliptic Cross-Section. *International Applied Mechanics*. 2021. 57. Pp. 282–289. DOI: 10.1007/s10778-021-01079-1
4. Raspopina, V., Perelygina, A., Shemetov, L., Grigorov, P. Dependence between the Mechanical Characteristics of the Material and the FDM Sample Made From This Material. *Safety in Aviation and Space Technologies. Select Proceedings of the 9th World Congress "Aviation in the XXI Century"*. Cham, 2022. Pp. 215–227. DOI: 10.1007/978-3-030-85057-9_18
5. Paimushin, V.N., Gazizullin, R.K., Polyakova, N.V., Shishov, M.A. Sandwich Shells with Composite Facings and a Transversally Flexible Core: Refined Equations and Buckling Modes of Specimens under Four-Point Bending Tests. *Advanced Structured Materials*. 2021. 141. Pp. 391–411. DOI: 10.1007/978-3-030-54928-2_29
6. Ubayduloev, M.N., Serazutdinov, M.N. Simulation and Calculation of Stress–Strain State of Thin-Walled Structures Strengthened under Load. *Lecture Notes in Mechanical Engineering*. 2022. Pp. 332–340. DOI: 10.1007/978-3-030-85233-7_40
7. Rozin, L.A. *Zadachi teorii uprugosti i chislennyye metody ikh resheniya* [Problems of the theory of elasticity and numerical methods for their solution]. St. Petersburg: Publishing house of SPbSTU, 1998. 531 p.
8. Klochkov, Y.V., Nikolaev, A.P., Vakhnina, O.V. Calculation of Rotation Shells Using Finite Triangular Elements with Lagrange Multipliers in Variative Approximation of Displacements. *Journal of Machinery Manufacture and Reliability*. 2016. 45 (1). Pp. 51–58. DOI: 10.3103/S1052618816010076
9. Leonetti, L., Magisano, D., Madeo, A., Garcea, G., Kiendl, J., Reali, A. A simplified Kirchhoff–Love large deformation model for elastic shells and its effective isogeometric formulation. *Computer Methods in Applied Mechanics and Engineering*. 2019. 354. Pp. 369–396. DOI: 10.1016/j.cma.2019.05.025
10. Lalin, V., Rybakov, V., Sergey, A. The finite elements for design of frame of thin-walled beams. *Applied Mechanics and Materials*. 2014. 578–579. Pp. 858–863. <https://doi.org/10.4028/www.scientific.net/amm.578-579.858>
11. Tyukalov, Yu.Ya. Quadrilateral Finite Element for Thin and Thick Plates. *Construction of Unique Buildings and Structures*. 2021. 5 (98). Pp. 9802. DOI: 10.4123/CUBS.98.2
12. Rozin, L.A., Terpugov, V.N. *Variatsionnyye zadachi uprugogo ravnovesiya s odnovremenno zadannymi skachkami napryazheniy i peremeshcheniy* [Variational problems of elastic equilibrium with simultaneously given jumps of stresses and displacements]. *Scientific and technical statements of the St. Petersburg State Polytechnic University*. 2009. 1 (74). Pp. 65–72. (rus)
13. Klochkov, Yu., Nikolaev, A., Vakhnina, O., Sobolevskaya, T., Klochkov, M. Physically Nonlinear Shell Deformation Based on Three-Dimensional Finite Elements. *Magazine of Civil Engineering*. 2022. 5 (113). Pp. 11314. DOI: 10.34910/MCE.113.14
14. Sultanov, L.U. Analysis of Finite Elasto-Plastic Strains: Integration Algorithm and Numerical Examples. *Lobachevskii Journal of Mathematics*. 2018. 39 (9). Pp. 1478–1483. DOI: 10.1134/S1995080218090056
15. Zheleznov, L.P., Kabanov, V.V., Boiko, D.V. Nonlinear Deformation and Stability of Discrete-Reinforced Elliptical Cylindrical Composite Shells under Torsion and Internal Pressure. *Russian Aeronautics*. 2018. 61 (2). Pp. 175–182. DOI: 10.3103/S1068799818020046
16. Bakulin, V.N. Model for Analysis of the Stress-Strain State of Three-Layer Cylindrical Shells with Rectangular Cutouts. *Mechanics of Solids*. 2022. 57 (1). Pp. 102–110. DOI: 10.3103/S0025654422010095
17. Agapov, V. The Family of Multilayered Finite Elements for the Analysis of Plates and Shells of Variable Thickness. *E3S Web of Conferences. 2018 Topical Problems of Architecture, Civil Engineering and Environmental Economics, TPACEE 2018*. 2019. Pp. 02013. DOI: 10.1051/e3sconf/20199102013
18. Lalin, V.V., Rybakov, V.A., Ivanov, S.S., Azarov, A.A. Mixed finite-element method in V.I. Slivker's semi-shear thin-walled bar theory. *Magazine of Civil Engineering*. 2019. 5 (89). P. 79–93. DOI: 10.18720/MCE.89.7
19. Magisano, D., Liang, K., Garcea, G., Leonetti, L., Ruess, M. An efficient mixed variational reduced-order model formulation for nonlinear analyses of elastic shells. *International Journal for Numerical Methods in Engineering*. 2018. 113 (4). Pp. 634–655. DOI: 10.1002/nme.5629
20. Garcea, G., Liguori, F.S., Leonetti, L., Magisano, D., Madeo, A. Accurate and efficient a posteriori account of geometrical imperfections in Koiter finite element analysis. *Int. J. Numer. Methods Eng.* 2017. 112 (9). Pp. 1154–1174. DOI: 10.1002/nme.5550
21. Yakupov, S.N., Kiyamov, H.G., Yakupov, N.M. Modeling a Synthesized Element of Complex Geometry Based Upon Three-Dimensional and Two-Dimensional Finite Elements. *Lobachevskii Journal of Mathematics*. 2021. 42 (9). Pp. 2263–2271. DOI: 10.1134/S1995080221090316
22. Novozhilov, V.V. *Teoriya tonkikh obolochek* [Theory of thin shells]. St. Petersburg: Publishing House of the St. Petersburg University, 2010. 378 p.
23. Rickards, R.B. *Metod konechnykh elementov v teorii obolochek i plastin* [Finite element method in the theory of shells and plates]. Riga: Known, 1988. 284 p.

24. Lei, Zh., Gillot, F., Jezeguel, L. Developments of the mixed grid isogeometric Reissner-Mindlin shell: serendipity basis and modified reduced. *Int. J. Mech.* 2015. 54. Pp. 105–119.
25. Pogorelov, A.V. *Differentsial'naya geometriya [Differential geometry]*. 6th ed., stereotype. Moscow: Nauka, 1974. 176 p.
26. Sedov, L.I. *Mekhanika sploshnoy sredy [Mechanics of a continuous medium]*. v. 1. Moscow: Nauka, 1976. 536 p.
27. Klochkov, Yu.V., Nikolaev, A.P., Sobolevskaya, T.A., Vakhnina, O.V., Klochkov, M.Yu. The calculation of the ellipsoidal shell based FEM with vector interpolation of displacements when the variable parameterisation of the middle surface. *Lobachevskii Journal of Mathematics*. 2020. 41 (3). Pp. 373–381. DOI: 10.1134/S1995080220030117
28. Postnov, V.A., Kharkhurim, I.Ya. *Metod konechnykh elementov v raschetakh sudovykh konstruktсий [Finite element method in calculations of ship structures]*. L. : Shipbuilding, 1974. 342 p.

Information about authors:

Yuriy Klochkov, Doctor of Technical Sciences

ORCID: <https://orcid.org/0000-0002-1027-1811>

E-mail: klotchkov@bk.ru

Valeria Pshenichkina, Doctor of Technical Sciences

ORCID: <https://orcid.org/0000-0001-9148-2815>

E-mail: vap_hm@list.ru

Anatoly Nikolaev, Doctor of Technical Sciences

ORCID: <https://orcid.org/0000-0002-7098-5998>

E-mail: anpetr40@yandex.ru

Olga Vakhnina, PhD in Technical Sciences

ORCID: <https://orcid.org/0000-0001-9234-7287>

E-mail: ovahnina@bk.ru

Mikhail Klochkov,

ORCID: <https://orcid.org/0000-0001-6751-4629>

E-mail: m.klo4koff@yandex.ru

Received 01.03.2023. Approved after reviewing 26.04.2023. Accepted 27.04.2023.